

## Acceptor-related photoluminescence study in GaAs/Ga<sub>1-x</sub>Al<sub>x</sub>As quantum wells

L. E. Oliveira

*Instituto de Física, Universidade Federal Fluminense, Outeiro de S.J. Batista s/n, Niterói, Caixa Postal 296, 24020 Rio de Janeiro, Rio de Janeiro, Brazil*  
 and *Instituto de Física, "Gleb Wataghin," Universidade Estadual de Campinas (UNICAMP), Caixa Postal 6165, 13081 Campinas, São Paulo, Brazil*

J. López-Gondar

*Instituto de Física, Universidade Federal Fluminense, Outeiro de S.J. Batista s/n, Niterói, Caixa Postal 296, 24020 Rio de Janeiro, Rio de Janeiro, Brazil*  
 and *Department of Theoretical Physics, University of Habana, San Lazaro y L. Vedado, Ciudad Habana, 10400, Cuba*  
 (Received 20 September 1989)

A theoretical study of the photoluminescence spectrum associated with shallow acceptors in GaAs-(Ga,Al)As quantum wells is performed. As a general feature, there are two special structures in the acceptor-related spectrum: an edge associated with transitions involving acceptors at the center of the well, and a peak associated with transitions related to on-edge acceptors. The photoluminescence line shape depends on the temperature, the quasi-Fermi energy of the conduction-subband electron gas, and on the acceptor distribution along the quantum well. It is suggested that an analysis of the acceptor-photoluminescence line shape could allow an experimental determination of the quasi-Fermi-energy level of the conduction-subband electron gas as well as of the on-edge-acceptor binding energy. Experimental results of unintentionally doped multiple-quantum-well GaAs-Ga<sub>0.7</sub>Al<sub>0.3</sub>As samples by Miller *et al.* [Phys. Rev. B **25**, 3871 (1982)] and of single quantum wells of GaAs-Ga<sub>0.85</sub>Al<sub>0.15</sub>As by Meynadier *et al.* [J. Appl. Phys. **58**, 4307 (1985)] are in excellent agreement with theoretical results obtained with a homogeneous distribution of acceptor impurities along the GaAs layer and a convenient choice of the quasi-Fermi-energy level.

### I. INTRODUCTION

Since the original proposal by Esaki and Tsu<sup>1</sup> on synthesized semiconductor superlattices, the advent of modern growth techniques such as molecular-beam epitaxy and metal-organic chemical-vapor deposition has made possible the realization of high-quality man-made systems consisting of alternating layers of two different semiconductors with controlled layer thicknesses and sharp interfaces between the layers. These so-called superlattices and heterostructures have been receiving considerable attention<sup>2-4</sup> in the last two decades due to the unique nature of their electronic states. The integral and fractional quantum Hall effects<sup>5-7</sup> observed in low-dimensional systems are spectacular examples of the new physics associated with these man-made structures.

Heterostructures consisting of alternating layers of Ga<sub>1-x</sub>Al<sub>x</sub>As ( $x < 0.4$ ) and GaAs, with thicknesses varying from a few atomic layers to several hundreds of Å, have been widely studied and present a band-gap discontinuity distributed approximately 60% on the conduction and 40% on the valence band.<sup>8,9</sup> Both electrons and holes in each GaAs layer of the heterostructure are confined in a potential well arising from the larger gap of the neighboring Ga<sub>1-x</sub>Al<sub>x</sub>As layers. Quantum size effects will occur and therefore the Ga<sub>1-x</sub>Al<sub>x</sub>As-GaAs-Ga<sub>1-x</sub>Al<sub>x</sub>As system is referred to as a quantum well (QW).

Due to the potential device applications of heterostructures,<sup>10-15</sup> the understanding of the properties of impurity states associated with such systems is a subject of considerable technological and scientific relevance. The first theoretical study in that area was performed by Bastard<sup>16</sup> on hydrogenic impurities in infinite-barrier QW's. In the past few years, several experimental and theoretical works have been reported on the subject of impurity states in low-dimensional systems and, in particular, on the properties of shallow donors and acceptors in GaAs-(Ga,Al)As QW's.

From the theoretical point of view, the effects of finite barriers on the on-center-donor binding energy in GaAs-Ga<sub>1-x</sub>Al<sub>x</sub>As QW's was studied by Greene and Bajaj,<sup>17</sup> whereas Mailhiot *et al.*<sup>18</sup> dealt with the problem of effective mass and dielectric-constant discontinuities at the interfaces for both the on-center and on-edge situations. The effect of nonparabolicity of the conduction band for an on-center donor in a finite QW was included by Chaudhuri and Bajaj.<sup>19</sup> The influence of a short-range core potential and of the  $\Gamma_8$  heavy-hole-light-hole valence-band coupling<sup>20,21</sup> on acceptor states and of spatially dependent screening<sup>22-24</sup> have also been considered in refining previous calculations.

Experimentally, Miller *et al.*<sup>25,26</sup> reported the first observation of impurity-related photoluminescence features which were attributed to the recombination of  $n=1$  conduction-subband electrons with neutral acceptors in

unintentionally doped<sup>25</sup> and Be-doped<sup>26</sup> molecular-beam-epitaxy (MBE)-grown GaAs-Ga<sub>1-x</sub>Al<sub>x</sub>As multiple QW's. Meynadier *et al.*<sup>27</sup> have also performed acceptor-related photoluminescence measurements in nominally undoped GaAs-Ga<sub>1-x</sub>Al<sub>x</sub>As QW's. Various experimental results on the properties of donors in GaAs-Ga<sub>1-x</sub>Al<sub>x</sub>As QW's have been reported by Shanabrook *et al.*<sup>28,29</sup> A detailed account of experimental and theoretical work in this field may be found in recent reviews.<sup>30-33</sup>

The acceptor binding energies measured by Miller *et al.*<sup>25</sup> were *quantitatively* interpreted by Masselink *et al.*<sup>20,21</sup> and Chang<sup>33,34</sup> with a calculation of the binding energies of *on-center* acceptors. Also, the experimentally measured donor binding energies were compared with theoretical calculations<sup>17,18,30</sup> involving *on-center* donors. Meynadier *et al.*<sup>27</sup> calculated the electron-to-acceptor photoluminescence line shape and claimed that the acceptor distribution which would fit their experimental results had its maximum, at the well interface, extending about 7 Å in the barrier and 12–30 Å in the well. As will be argued in this work, the various observed photoluminescence spectra are not related to impurities exclusively at the on-center position. The distribution of acceptors centered around the on-edge location, proposed by Meynadier *et al.*,<sup>27</sup> is not necessarily the adequate one. In fact, the experimental results should be compared with a theoretical impurity-related photoluminescence spectrum calculated for a given distribution of impurities along the heterostructure and depending not only on the temperature but also on the quasi-Fermi energy of the conduction-subband electron gas.<sup>35</sup>

In this work we analyze the theoretical photoluminescence spectrum associated with transitions between the  $n=1$  conduction subband electron gas and the acceptor-impurity band for a GaAs-Ga<sub>1-x</sub>Al<sub>x</sub>As QW. Section II will present some theoretical aspects on the calculation of the photoluminescence spectra. Results and discussion are in Sec. III, and conclusions are in Sec. IV.

## II. THEORY

The transition probability per unit time from initial ( $i$ ) conduction states to a final ( $f$ ) acceptor state is given by<sup>36</sup>

$$W = \frac{2\pi}{\hbar} \sum_i |\langle f | H_{\text{int}} | i \rangle|^2 \delta(E_f - E_i - \hbar\omega), \quad (2.1)$$

where  $H_{\text{int}} = C\mathbf{e} \cdot \mathbf{p}$ ,  $\mathbf{e}$  is the polarization vector in the direction of the electric field of the radiation,  $\mathbf{p}$  is the momentum operator, and  $C$  is a prefactor which contains the photon vector potential. The matrix elements may be written as<sup>36,37</sup>

$$\begin{aligned} \langle f | H_{\text{int}} | i \rangle &\simeq C \left[ \frac{1}{\Omega} \int_{\Omega} d\mathbf{r} u_f^*(\mathbf{r}) \mathbf{e} \cdot \mathbf{p} u_i(\mathbf{r}) \right] \\ &\times \left[ \int d\mathbf{r} F_f^*(\mathbf{r}) F_i(\mathbf{r}) \right], \end{aligned} \quad (2.2)$$

where  $\Omega$  denotes the volume of the unit cell,  $u_f$  ( $u_i$ ) is the periodic part of the Bloch state for the final (initial) state, and  $F_f$  ( $F_i$ ) is the envelope function for the final (initial) state.

For a GaAs-(Ga,Al)As QW of width  $L$ , the transition probability per unit time for conduction-subband to acceptor (associated with a single impurity located at  $z = z_i$ ; the  $z=0$  origin is chosen at the center of the GaAs well) transitions is therefore given by

$$\begin{aligned} W_L(z_i, \omega) &= W_0 \frac{1}{2} \left[ \frac{a_0^*}{a_0} \right]^2 \left[ \frac{m_c^*}{m_0} \right] (N_b^2 a_0^*) \frac{N^2 J^2}{a_0^{*3}} \Big|_{k_{\perp}(z_i)} \\ &\times Y(\hbar\omega - \varepsilon_g + E(L, z_i)), \end{aligned} \quad (2.3)$$

where  $a_0$  is the Bohr radius,  $m_0$  is the free-electron mass,  $a_0^* = \hbar^2 \varepsilon_0 / (m_v^* e^2)$  is the effective Bohr radius associated with the acceptor impurity,  $Y(x)$  is the step function,  $N = (1 / \langle \Psi | \Psi \rangle)^{1/2}$  is the normalization factor for the acceptor variational<sup>24</sup> wave function, and  $N_b$  is the normalization factor for the wave function associated with the first conduction subband. In the above expression, we have

$$k_{\perp}(z_i) = \{ 2m_c^* [\hbar\omega - \varepsilon_g + E(L, z_i)] / \hbar^2 \}^{1/2}, \quad (2.4a)$$

$$\varepsilon_g = E_g + E_{n=1}^c + E_{n=1}^v, \quad (2.4b)$$

$$W_0 = \frac{4m_0}{\hbar^3} a_0^2 |C|^2 |\mathbf{e} \cdot \mathbf{P}_{\hbar}|^2, \quad (2.4c)$$

in which  $E_g$  is the bulk GaAs gap,<sup>38</sup>  $E_{n=1}^c$  ( $E_{n=1}^v$ ) is the bottom (top) of the first conduction (valence) subband,  $E(L, z_i) = E_i$  is the acceptor binding energy, and  $\mathbf{e} \cdot \mathbf{P}_{\hbar}$  is the first RHS matrix element in Eq. (2.2). One should point out that the coupling between the top four valence bands<sup>20</sup> is neglected and it was considered a spherical heavy-hole effective mass  $m_v^* \simeq 0.30m_0$  which gives a bulk value<sup>25</sup> of 26 meV for the effective Rydberg  $R_0^* = m_v^* e^4 / (2\hbar^2 \varepsilon_0^2)$ . Also, although the effective masses,  $m_{v,c}^*$ , and the dielectric constant vary across the interfaces,<sup>18</sup> we assume the values of  $m_{v,c}^*$  and of the dielectric constant in GaAs for all regions of the heterostructure.

In the case of a rectangular GaAs-(Ga,Al)As finite QW with its growth direction along the  $z$  axis, we have<sup>39</sup> for  $J = J(z_i, \lambda, k_{\perp}(\omega))$  in Eq. (2.3) [ $J$  is related to the second RHS matrix element in Eq. (2.2)],

$$J = 2\pi(L/2)^4 \frac{1}{\lambda\mu^3} \left[ \Phi - \mu \frac{\partial \Phi}{\partial \mu} \right], \quad (2.5)$$

where  $\lambda$  is the variational parameter of the acceptor wave function,

$$\Phi = e^{-\mu} \cosh(2\mu z_i/L) \left[ \frac{2}{\gamma_1 + \mu} + \alpha \alpha_b \frac{-\mu \cos(\gamma_+) + \gamma_+ \sin(\gamma_+)}{\gamma_+^2 + \mu^2} + \alpha \alpha_b \frac{-\mu \cos(\gamma_-) + \gamma_- \sin(\gamma_-)}{\gamma_-^2 + \mu^2} \right] + \alpha \alpha_b \left[ \frac{\mu \cos(2\gamma_+ z_i/L)}{\gamma_+^2 + \mu^2} + \frac{\mu \cos(2\gamma_- z_i/L)}{\gamma_-^2 + \mu^2} \right], \quad (2.6)$$

and

$$\mu = (k_1^2 + \lambda^{-2})^{1/2} L / 2, \quad (2.7a)$$

$$\gamma_{\pm} = (k_2 \pm k_{2b}) L / 2, \quad (2.7b)$$

$$\gamma_1 = (k_1 + k_{1b}) L / 2, \quad (2.7c)$$

$$k_1 = [2m_v^*(V_B - E_0)]^{1/2} / \hbar, \quad (2.7d)$$

$$k_2 = (2m_v^* E_0)^{1/2} / \hbar, \quad (2.7e)$$

$$\alpha = 1 / \cos(k_2 L / 2). \quad (2.7f)$$

In the above expressions  $k_{1b}$ ,  $k_{2b}$ , and  $\alpha_b$  are given by Eqs. (2.7d), (2.7e), and (2.7f) with the effective mass and barrier potential  $V_B$  corresponding to the conduction subband. We assume<sup>24</sup> that the band-gap discontinuity<sup>8,9</sup> in the GaAs-Ga<sub>1-x</sub>Al<sub>x</sub>As heterostructure is distributed about 40% on the valence band and 60% on the conduction band with the total band-gap difference  $\Delta E_g$  between GaAs and Ga<sub>1-x</sub>Al<sub>x</sub>As given as a function of the Al concentration  $x < 0.4$  as<sup>40</sup>  $\Delta E_g$  (eV) = 1.247 $x$ .

We now consider a single QW with a  $N_a(z_i)$  distribu-

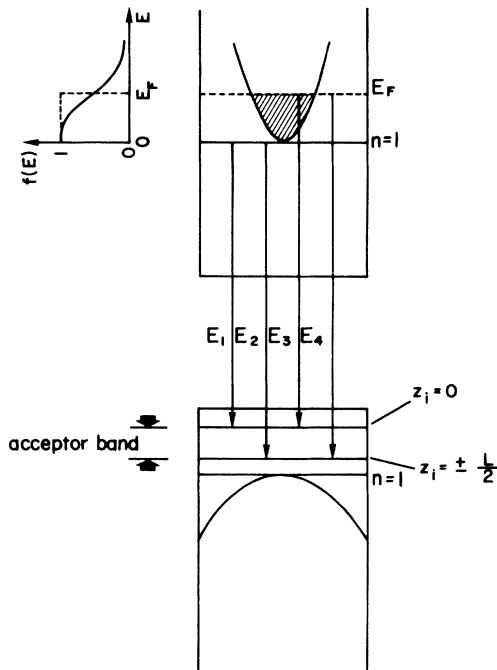


FIG. 1. Schematic representation of special luminescence transitions in a GaAs-(Ga,Al)As QW with an acceptor impurity band. The parabolas represent a pictorial view of the planar ( $k_{\perp}$  dependence) dispersion of the first conduction and valence subbands. Also shown is the Fermi distribution for the conduction-subband electron gas.

tion of acceptor hydrogenic impurities in which electrons have been optically injected into the conduction band and recombine with holes in the acceptor or valence bands (see Fig. 1). We are concerned with the line shape of the recombination associated with holes in the acceptor band and we assume that the temperature is low enough ( $T \ll 100$  K) such that each acceptor state is filled with a hole. The photoluminescence spectrum associated with the  $n=1$  conduction-subband to acceptor transitions is therefore given by

$$L(\omega) = (1/L) \int_{-L/2}^{L/2} dz_i N_a(z_i) W_L(z_i, \omega) f(\epsilon_{k_1}), \quad (2.8)$$

where  $f(\epsilon_{k_1}) = 1 / \{1 + \exp[\beta(\hbar\omega - \epsilon_g + E_i - E_F)]\}$  is the Fermi distribution ( $\beta = 1/k_B T$ ) for the conduction-subband electron gas, and  $E_F$  is the quasi-Fermi energy level (measured from the bottom of the subband) of the electron gas in the steady-state quasiequilibrium.

### III. RESULTS AND DISCUSSION

Calculations were performed for GaAs QW's of infinite depth as well as for GaAs-Ga<sub>1-x</sub>Al<sub>x</sub>As QW's with different Al concentrations. Unless otherwise stated, the results in this work assume a homogeneous<sup>16</sup> distribution of acceptors along the well (e.g.,  $N_a(z_i) = 1$ ). The acceptor-related theoretical photoluminescence spectra for a  $L/a_0^* = 1$  infinite QW and  $m_v^*/m_c^* = 6$  are shown in Fig. 2 for different quasi-Fermi energies and a temperature such that  $\beta E_{\max}^i = 23$ , where  $E_{\max}^i$  is the on-center acceptor binding energy. Our results should be compared with those of Fig. 8 of the work by Bastard.<sup>16</sup> No-

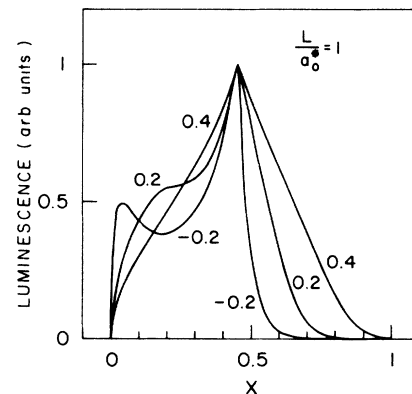


FIG. 2. Luminescence spectra for an infinite QW associated with electron  $\rightarrow$  acceptor-band recombinations for three different quasi-Fermi energies:  $E_F/E_{\max}^i = -0.2, 0.2,$  and  $0.4$ , with  $L/a_0^* = 1$ ,  $\beta E_{\max}^i = 23$ , and  $m_v^*/m_c^* = 6$ . The curves are scaled to reach 1 at their maxima. The quantity plotted on the horizontal axis is given by  $\hbar\omega = \epsilon_g - E_{\max}^i + x E_{\max}^i$ .

tice that, in our results, the photoluminescence spectra go continuously to zero as  $x \rightarrow 0^+$ , as expected,<sup>39</sup> whereas Bastard obtained a steplike behavior for  $L(\omega)$ .

Figure 3 displays our results for the photoluminescence spectra in  $L = 20\text{-}\text{\AA}$  GaAs-(Ga,Al)As QW's at  $T = 25\text{ K}$  and with typical<sup>16,41,42,43</sup> quasi-Fermi-energy levels of the conduction-subband electron gas of  $E_F = 20, 10,$  and  $-10$  meV, respectively. Some characteristic features should be pointed out. The spectra present two van Hove-like structures at  $E_1(E'_1)$  and  $E_2(E'_2)$  associated with special

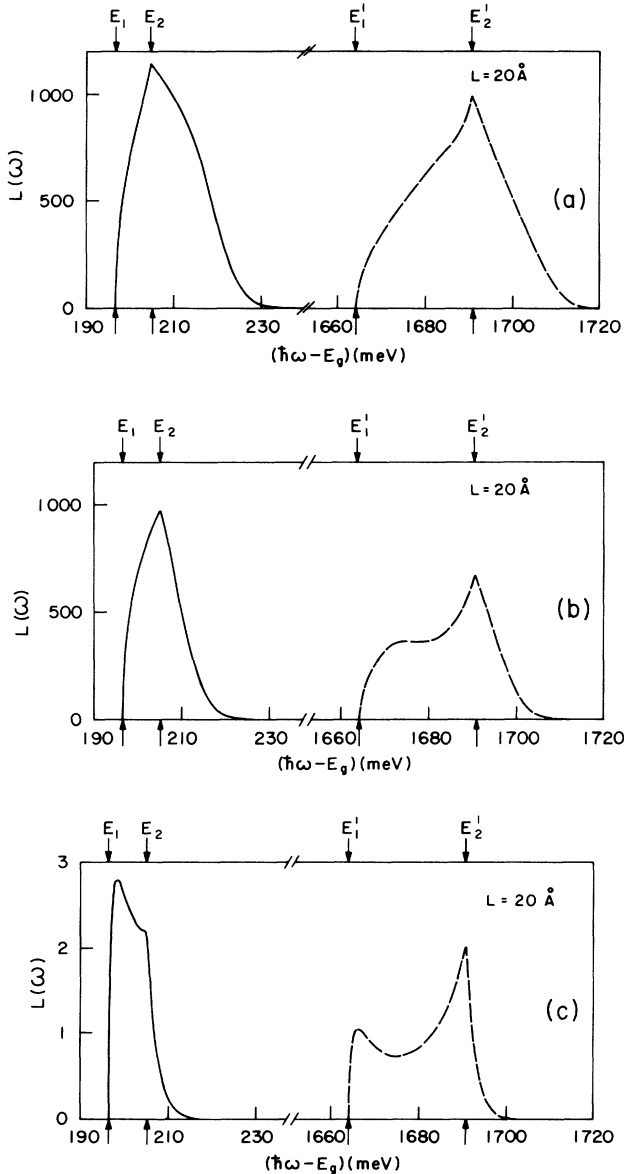


FIG. 3. Photoluminescence line shape (in unites of  $W_0$ ; see text) associated with electron-to-acceptor recombinations for a  $L = 20\text{-}\text{\AA}$  GaAs-(Ga,Al)As QW,  $T = 25\text{ K}$ , and three different quasi-Fermi energies: (a)  $E_F = 20$  meV, (b)  $E_F = 10$  meV, and (c)  $E_F = -10$  meV. The dashed lines correspond to an infinite-barrier GaAs QW and full curves to a GaAs- $\text{Ga}_{0.7}\text{Al}_{0.3}\text{As}$  QW.  $E_1$  and  $E'_1$  ( $E_2$  and  $E'_2$ ) indicate the onset of transitions from the conduction subband to the upper edge (lower edge) of the acceptor band.  $E_g$  is the bulk GaAs gap.

transitions from the bottom of the conduction subband to states corresponding to acceptors at the on-center and on-edge positions, respectively. Therefore, a measurement of the luminescence spectra associated with acceptors would, in principle, allow a determination of the on-edge and on-center acceptor binding energies. The shift of the finite-barrier luminescence curves to smaller energies when compared to the infinite case is essentially due to changes in the  $n = 1$  conduction- and valence-subband edges when the finite-barrier potential is considered. This behavior is similar to the one found when studying the optical absorption spectra<sup>39</sup> associated with impurities in QW's. It is also apparent from Fig. 3 that changes in the quasi-Fermi-energy level (which depends essentially on the experimental conditions such as the laser power and frequency, electron-phonon scattering rates, etc.) may considerably change<sup>35</sup> the photoluminescence spectrum.

The acceptor-related luminescence spectra for a  $L = 100\text{-}\text{\AA}$  GaAs- $\text{Ga}_{0.7}\text{Al}_{0.3}\text{As}$  QW is presented in Fig. 4 for  $E_F = 10$  meV and two different temperatures,  $T = 2$  and  $25\text{ K}$ . At  $T = 2\text{ K}$  the van Hove-like structures  $E_3$  and  $E_4$  (cf. Fig. 1) clearly show up in the spectrum. The structure at  $E_3$  is related to transitions from the quasi-Fermi-energy level of the conduction-subband-electron gas to states associated with on-center acceptor impurities and becomes very much pronounced at  $T = 2\text{ K}$ , suggesting<sup>35</sup> the possibility of performing precise photoluminescence measurements of the quasi-Fermi-energy level of the conduction electron gas in the steady-state quasiequilibrium. One should note that the photoluminescence spectra associated with the shallow acceptor band would in general appear in the low-energy "tail" of the excitonic line, which was not considered in this work and, therefore, the features connected to the van Hove-like structures  $E_1$  and  $E_4$  would be very difficult to be experimentally observed.

Of course, the impurity-related photoluminescence

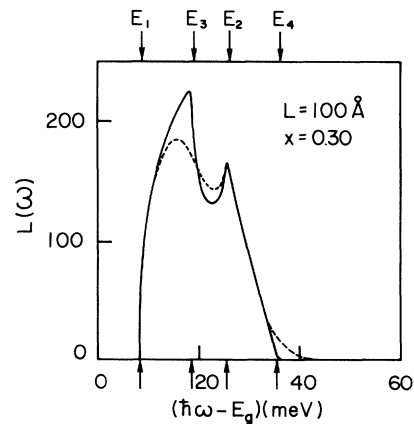


FIG. 4. Luminescence spectra (in units of  $W_0$ ; see text) of shallow acceptors for an  $L = 100\text{-}\text{\AA}$  GaAs- $\text{Ga}_{0.7}\text{Al}_{0.3}\text{As}$  QW,  $E_F = 10$  meV, and  $T = 2\text{ K}$  (solid curve) or  $T = 25\text{ K}$  (dashed line).  $E_1$  ( $E_2$ ) indicates the onset of transitions from the conduction subband to the upper edge (lower edge) of the acceptor band, and  $E_3$  and  $E_4$  indicate "critical" transitions associated with the quasi-Fermi level.

spectrum should depend not only on the quasi-Fermi-energy level (Fig. 3) and temperature (Fig. 4) but also on the distribution of acceptors along the well. Shanabrook and Comas<sup>28</sup> have performed photoluminescence experiments from "spike-doped" hydrogenic donors at the center of (Ga,Al)As-GaAs QW's with the width of the doping spike of the order of 50 Å as compared to nominally undoped samples, and the results indicated considerable changes in the luminescence line shape. We therefore investigated the effect on the acceptor-related photoluminescence spectrum of a Gaussian (centered at  $z_i=0$  and with a 50-Å halfwidth) distribution of acceptors inside the well as compared to the homogeneous one. The results are shown in Fig. 5 for a  $L=160$ -Å  $\text{Ga}_{0.7}\text{Al}_{0.3}\text{As}$ -GaAs QW and for various quasi-Fermi energy levels, and indicate the qualitative differences in the spectrum from different distributions of impurities. Our theoretical results in Fig. 5 should be compared with the smaller peak (extrinsic luminescence) in the photoluminescence spectrum of Fig. 1 by Miller *et al.*<sup>25</sup>

Results presented up to Fig. 5 have been calculated with a constant  $\epsilon_0$  screening<sup>16</sup> for the hydrogenic impurity potential. In dealing with impurity states, however, it can be argued that a more realistic description of screening can be achieved with a spatially dependent  $\epsilon(r)$  dielectric response,<sup>23,24</sup> and therefore, from now on and in order to compare our results with experimental data we will use such an approach. For acceptor-impurity states, spatially dependent screening effects<sup>23,24</sup> may shift the impurity binding energies up to a few meV for QW widths of the order of  $\approx 100$  Å.

In order to analyze the experimental acceptor-related photoluminescence results by Miller *et al.*<sup>25</sup> in unintentionally doped multiple QW's of (Ga,Al)As-GaAs, we have performed calculations (for a homogeneous distribution of acceptor impurities along the QW) of the acceptor-luminescence spectra of a  $L=50$ -Å GaAs- $\text{Ga}_{0.7}\text{Al}_{0.3}\text{As}$  single QW at  $T=5$  K and quasi-Fermi energies of  $E_F=5, 10,$  and  $20$  meV (cf. Fig. 6). For  $E_F \approx 5$ – $10$  meV, we find a double-peaked structure in the theoretical luminescence spectra in agreement with the  $L=50$  Å experimental results by Miller *et al.*<sup>25</sup> Notice that one of the peaks in the theoretical spectra is associated with on-edge acceptors (cf. Fig. 6 and  $E_2$  van Hove-like structure). Moreover, for  $E_F=5$  meV, the energy difference between the two peaks in the luminescence spectra is in excellent agreement with experimental data.<sup>25</sup> Figure 7 shows the calculated spectra for  $E_F=5$  meV and different GaAs-(Ga,Al)As QW widths. One should notice that the relative weight of the  $E_2$  on-edge acceptor-related luminescence peak with respect to the other peak decreases with increasing QW widths. Therefore, it is apparent from Fig. 7 that the  $E_2$  peak (associated with the lower curve in Fig. 8) will be more difficult to be experimentally observed with increasing QW widths (for  $L > 100$  Å, the  $E_2$  structure is therefore indicated in Fig. 8 by a dashed curve); moreover, this difficulty will be increased because the  $E_2$  structure would appear in the tail of the exciton line (which is not accounted for in our theoretical calculation). Considering that, one should

note the rather good agreement—notice that<sup>38</sup>  $E_g=1.519$  eV—between our results in Fig. 7(b) and the spectrum corresponding to the smaller peak (extrinsic luminescence) in the photoluminescence spectrum of Fig.

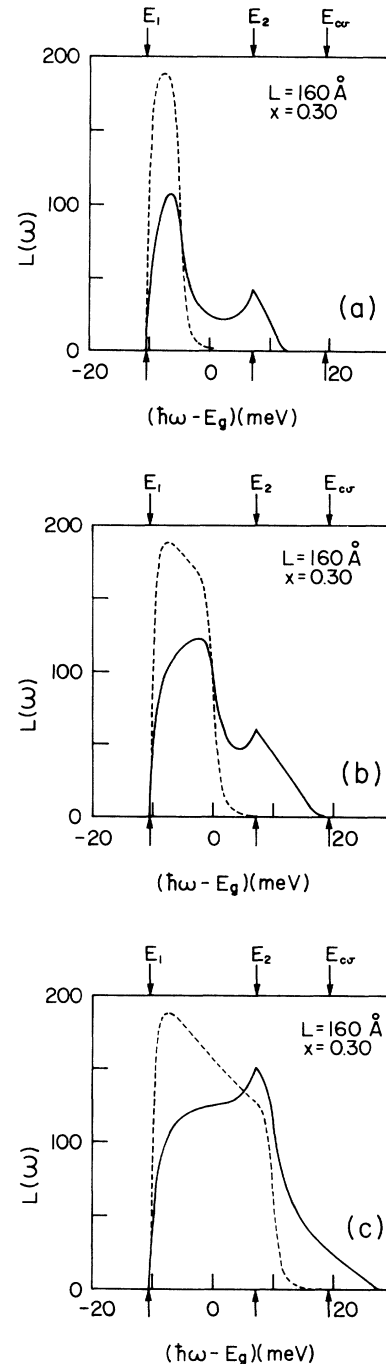


FIG. 5. Photoluminescence line shape (in units of  $W_0$ ; see text) associated with electron-to-acceptor recombinations for a  $L=160$ -Å  $\text{GaAs-Ga}_{0.7}\text{Al}_{0.3}\text{As}$  QW,  $T=5$  K, and quasi-Fermi energies (a)  $E_F=5$  meV, (b)  $E_F=10$  meV, and (c)  $E_F=20$  meV. The solid (dashed) curves correspond to a uniform (on-center Gaussian) distribution of acceptor impurities.  $E_1$  and  $E_2$  indicate the onset of transitions from the conduction subband to the upper and lower edges of the acceptor band, respectively, and  $E_{cv}$  the onset of conduction-to-valence subband transitions.

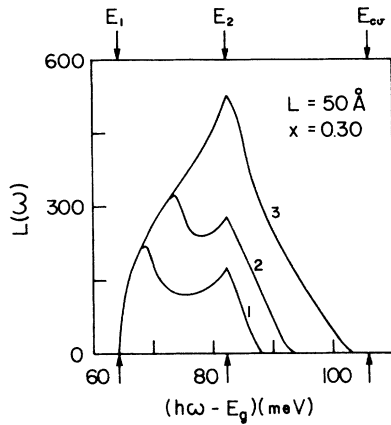


FIG. 6. Photoluminescence line shapes (in units of  $W_0$ ; see text) associated with electron-to-acceptor recombinations for a  $L=50\text{-}\text{\AA}$  GaAs-Ga<sub>0.7</sub>Al<sub>0.3</sub>As QW,  $T=5\text{ K}$ , and quasi-Fermi energies  $E_F=5\text{ meV}$  (curve 1),  $E_F=10\text{ meV}$  (curve 2), and  $E_F=20\text{ meV}$  (curve 3).  $E_1$  and  $E_2$  indicate the onset of transitions from the conduction subband to the upper and lower edges of the acceptor band, respectively, and  $E_{cv}$  the onset of conduction-to-valence subband transitions.

1 by Miller *et al.*<sup>25</sup>

The theoretical shifts  $\Delta E$  of the two peaks in the theoretical acceptor-related photoluminescence spectra with respect to  $E_{cv}$  (the onset of conduction-to-valence subband transitions) is displayed in Fig. 8 as functions of the GaAs-Ga<sub>0.7</sub>Al<sub>0.3</sub>As QW width for  $T=5\text{ K}$  and  $E_F=5\text{ meV}$ . Also shown are the experimental results for the so-called acceptor “binding energies” by Miller *et al.*<sup>25</sup> obtained in the same way. As is clear from our results in Figs. 7 and 8, the appropriate way to quantitatively compare theoretical and experimental “binding energies” from impurity-related photoluminescence results is via a careful analysis of the theoretical luminescence line shape and not through a calculation of on-center impurity binding energies as done in previous theoretical work.<sup>17,18,20,21,30,33,34</sup> Moreover, as mentioned before, one should be aware that the theoretical calculation depends considerably not only on the distribution of impurities along the heterostructure but also on the choice for the quasi-Fermi-energy level for the  $n=1$  conduction-subband electron gas. Since the experimental results<sup>25</sup> are for unintentionally doped QW samples, we have chosen a homogeneous distribution of acceptor impurities inside the QW. On the other hand, the choice for the conduction-subband quasi-Fermi-energy level ( $E_F=5\text{ meV}$ ) was essentially based on a comparison of the double-peaked theoretical photoluminescence results and experimental data for the “binding energies” in the case of a  $L=50\text{-}\text{\AA}$  GaAs-Ga<sub>0.7</sub>Al<sub>0.3</sub>As QW. An *ab initio* calculation of the quasi-Fermi-energy level of the conduction-subband electron gas for a given experimental situation is beyond the scope of this work.

Figure 9 displays the  $T=2\text{ K}$  acceptor-related theoretical photoluminescence spectra for GaAs-Ga<sub>1-x</sub>Al<sub>x</sub>As QW's with  $x=0.15$ , well widths of 50, 100, and 150  $\text{\AA}$ ,

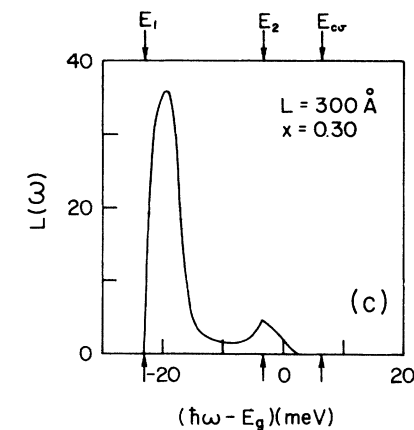
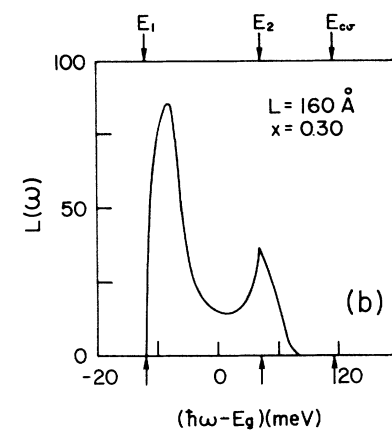
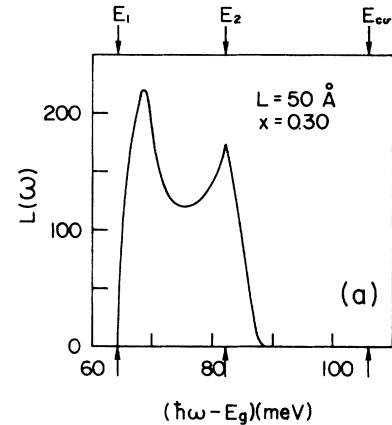


FIG. 7. Photoluminescence line shapes (in units of  $W_0$ ; see text) associated with electron-to-acceptor recombinations for a (a)  $L=50\text{-}\text{\AA}$ , (b)  $L=160\text{-}\text{\AA}$ , and (c)  $L=300\text{-}\text{\AA}$  GaAs-Ga<sub>0.7</sub>Al<sub>0.3</sub>As QW at  $T=5\text{ K}$  and quasi-Fermi energy  $E_F=5\text{ meV}$ .  $E_1$  and  $E_2$  indicate the onset of transitions from the conduction subband to the upper and lower edges of the acceptor band, respectively, and  $E_{cv}$  the onset of conduction-to-valence subband transitions.

and quasi-Fermi-energy levels of 5, 10, and 20 meV. The motivation for the calculation was the experimental results by Meynadier *et al.*<sup>27</sup> in nominally undoped GaAs-GaAlAs QW's. In all theoretical spectra one observes a well-defined structure at  $E_2$ , i.e., at the onset of transitions from the conduction subband to on-edge acceptor

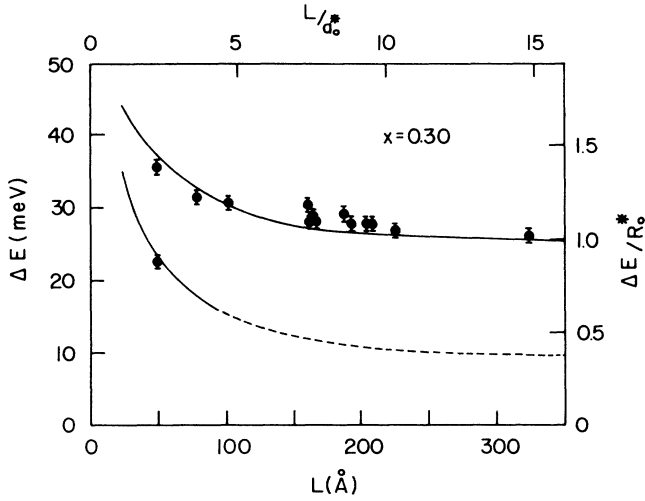


FIG. 8. Experimental binding energies (Ref. 25) versus quantum-well thickness  $L$  compared with theoretical curves associated with the two peaks of the  $T=5$  K photoluminescence spectra for GaAs-Ga<sub>0.7</sub>Al<sub>0.3</sub>As QW's with quasi-Fermi energy  $E_F=5$  meV.

states. This structure at  $E_2$  is clearly the relevant feature of the spectra for  $E_F=20$  meV. For  $E_F=5$  and 10 meV, however, the luminescence spectra present a dominant peak at the  $E_3$  van Hove-like structure (cf. Fig. 1) which is related to transitions from the quasi-Fermi-energy level of the  $n=1$  conduction-subband electron gas to states associated with on-center acceptors. Figure 10 then shows the theoretical shift with respect to  $E_{cv}$  of the main peak in the acceptor-related  $T=2$  K photoluminescence spectra for quasi-Fermi levels of  $E_F=10$  and 20 meV compared with the corresponding experimental results<sup>27</sup> for GaAs-Ga<sub>0.85</sub>Al<sub>0.15</sub>As QW's. The agreement between the experimental "binding energies" and the theoretical values associated with the  $E_2$  structure (related to on-edge acceptors) with  $E_F=20$  meV is rather good. Also, a comparison of our results in curve 3 of Fig. 9(a)—using<sup>38</sup>  $E_g=1.519$  eV—with the acceptor-related photoluminescence spectrum for  $L=50$  Å in Fig. 1 of Meynadier *et al.*<sup>27</sup> shows quite good agreement. As mentioned before, Meynadier *et al.*<sup>27</sup> have calculated<sup>44</sup> the electron-to-acceptor photoluminescence spectra for an acceptor distribution around the on-edge location and have argued that the impurities should extend about 7 Å inside the barrier and from 12–30 Å in the well in order to fit their experimental results. Our results in Figs. 9 and 10—calculated for an homogeneous distribution of acceptors inside the QW—indicate that the distribution of acceptors proposed by Meynadier *et al.*<sup>27</sup> and centered around the on-edge location is not necessarily the adequate one.

Photoluminescence experiments by Miller *et al.*<sup>26</sup> for a Be-doped GaAs-Al<sub>0.22</sub>Ga<sub>0.78</sub>As heterostructure at 5 K with 40 46-Å-wide GaAs QW's revealed a luminescence spectrum with a double-peak acceptor-related feature. The QW's were MBE-grown and doped throughout with

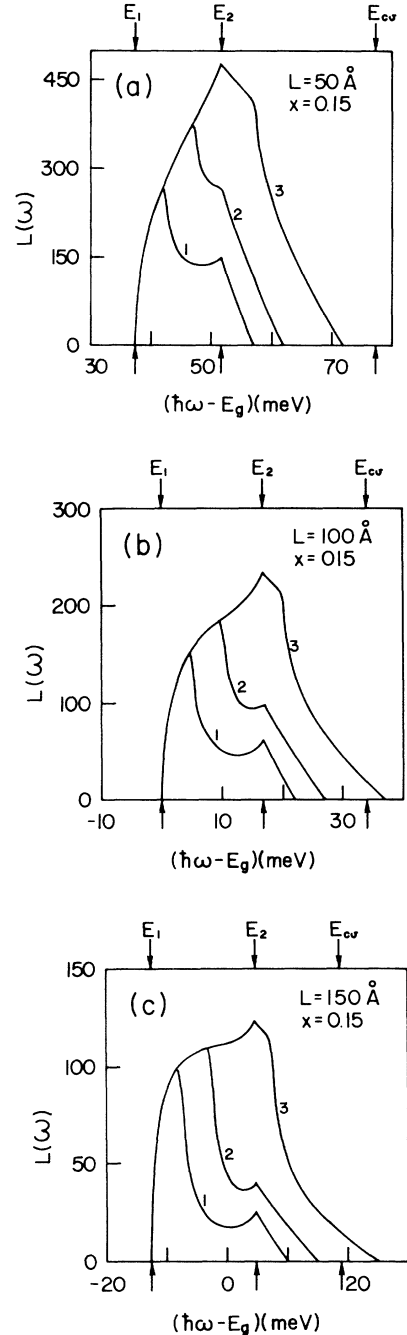


FIG. 9. Photoluminescence spectra (in units of  $W_0$ ; see text) associated with electron-to-acceptor recombinations for (a)  $L=50$ -Å, (b)  $L=100$ -Å, and (c)  $L=150$ -Å GaAs-Ga<sub>0.85</sub>Al<sub>0.15</sub>As QW's, with quasi-Fermi energies  $E_F=5$  meV (curve 1),  $E_F=10$  meV (curve 2), and  $E_F=20$  meV (curve 3), and  $T=2$  K.  $E_1$  and  $E_2$  indicate the onset of transitions from the conduction subband to the upper and lower edges of the acceptor band, respectively, and  $E_{cv}$  the onset of conduction-to-valence subband transitions.

Be. The double-peaked structure (with corresponding experimental "binding energies" of 22 and 46 meV) was interpreted as associated with Be<sup>0</sup> impurities both at the heterostructure interfaces and near the center of the

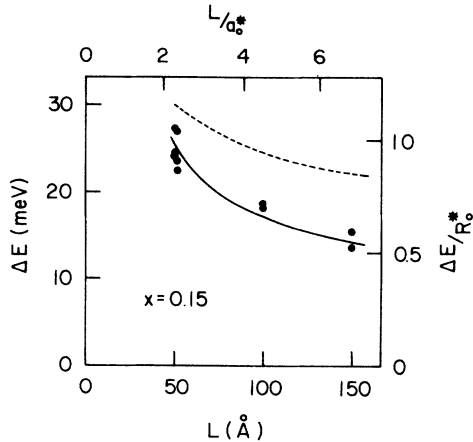


FIG. 10. Experimental binding energies (Ref. 27) versus quantum-well thickness  $L$  compared with theoretical results associated with the main peak of the  $T=2$  K photoluminescence spectra for GaAs-Ga<sub>0.85</sub>Al<sub>0.15</sub>As QW's with quasi-Fermi energies  $E_F=20$  meV (solid curve) and  $E_F=10$  meV (dashed curve).

wells. As stated by Miller *et al.*,<sup>26</sup> their results compared very well with the corresponding (21 and 47 meV, respectively) theoretical binding energies obtained by Bastard<sup>16</sup> based on an infinite potential QW. In order to investigate the photoluminescence line shape, we have performed the calculations of the luminescence spectra for the cases of both the infinite and finite potential QW's (see Fig. 11). We assumed an homogeneous (the QW's were doped throughout with Be by Miller *et al.*<sup>26</sup>) distribution of impurities inside the QW and a quasi-Fermi-energy level of 5 meV. Although the theoretical photoluminescence line shape and energy shift between the two

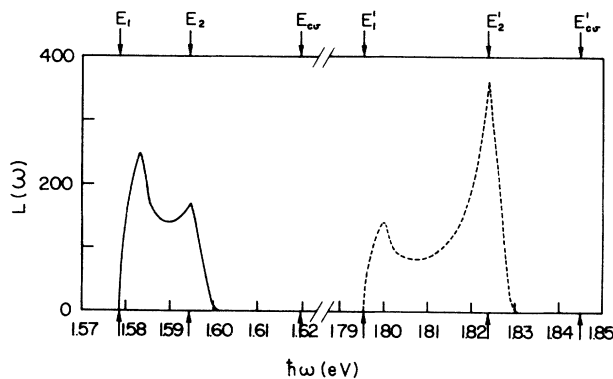


FIG. 11. Photoluminescence line shape (in units of  $W_0$ ; see text) associated with electron-to-acceptor recombinations for a  $L=46$ -Å GaAs-(Ga,Al)As QW,  $T=5$  K, and quasi-Fermi energy  $E_F=5$  meV. The dashed line corresponds to an infinite-barrier GaAs QW, and the solid curve to a GaAs-Ga<sub>0.78</sub>Al<sub>0.22</sub>As QW.  $E_1$  and  $E'_1$  ( $E_2$  and  $E'_2$ ) indicate the onset of transitions from the conduction subband to the upper edge (lower edge) of the acceptor band.  $E_{cv}$  ( $E'_{cv}$ ) indicates the onset of conduction  $\rightarrow$  valence intersubband transitions.

peaks in the infinite QW case are in agreement with experiment, the theoretical curve (in the infinite barrier case) is blue-shifted more than 200 meV with respect to the experimental spectrum. For the case of the finite-barrier QW, the calculated results are in the same energy range of the experimental results (cf. Fig. 1 of Miller *et al.*<sup>26</sup>) with the lower energy peak in fair agreement with the observed spectra. However, it is apparent from Fig. 11 that the theoretical on-edge peak ( $E_2$  structure) is about 10-meV red-shifted from experiment and with a weaker intensity than the lower-energy peak in contrast with the reported spectra. We believe these discrepancies are related to the following: (i) the calculated acceptor-related photoluminescence spectrum is for a single isolated QW whereas the experiment was performed in a multiple-quantum-well heterostructure with thin (50 Å) GaAlAs barriers; (ii) for such narrow ( $L=46$  Å) GaAs QW's small variations of the nominal well widths can cause appreciable shifts in the calculated spectrum (cf. Fig. 12 with spectra calculated for  $L=44, 46,$  and  $48$  Å); and, finally (iii) it was assumed a quasi-Fermi-energy level of 5 meV and an homogeneous distribution of acceptor impurities which may not be adequate to reproduce the experimental situation. It is clear, therefore, that more impurity-related photoluminescence measurements and theoretical work are certainly necessary if one is interested in an adequate quantitative description of the acceptor-related luminescence spectra of multiple QW's intentionally doped samples with such thin layers.

#### IV. CONCLUSIONS

In this work we performed a theoretical and systematic study of the photoluminescence spectrum associated with shallow acceptors in GaAs-(Ga,Al)As quantum wells. We observed, as a general feature, two special structures in the acceptor-related spectrum: an edge associated with transitions involving acceptors at the center of the well, and a peak associated with transitions related to on-edge acceptors. The photoluminescence line shape de-

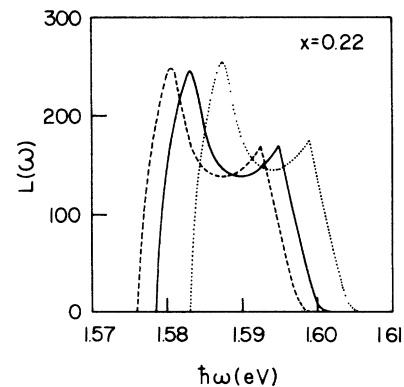


FIG. 12. Photoluminescence spectra (in units of  $W_0$ ; see text) associated with electron-to-acceptor recombinations for  $L=44$ -Å (dotted curve),  $L=46$ -Å (solid curve), and  $L=48$ -Å (dashed curve) GaAs-Ga<sub>0.78</sub>Al<sub>0.22</sub>As QW's with quasi-Fermi energy  $E_F=5$  meV, and  $T=5$  K.



depends on the temperature, the quasi-Fermi energy of the conduction-subband electron gas, and on the acceptor distribution along the quantum well. It is suggested that a careful analysis of the acceptor-photoluminescence line shape could allow an experimental determination of the quasi-Fermi-energy level of the conduction-subband electron gas as well as of the on-edge acceptor binding energy. Experimental results of unintentionally doped multiple-quantum-well GaAs-Ga<sub>0.7</sub>Al<sub>0.3</sub>As samples by Miller *et al.*<sup>25,26</sup> and of single quantum wells of GaAs-Ga<sub>0.85</sub>Al<sub>0.15</sub>As by Meynadier *et al.*<sup>27</sup> compared rather well with theoretical results obtained with a homogeneous distribution of acceptor impurities along the GaAs layer, provided that an adequate choice is made for the quasi-Fermi-energy level associated with the  $n = 1$  conduction-subband electron gas.

We emphasize that impurity-related experimental photoluminescence measurements in QW's, multiple QW's, and heterostructures should be compared with the corresponding impurity-related theoretical luminescence spectrum which considerably depends on the distribution of

impurities along the heterostructure and on the quasi-Fermi-energy level of the conduction-subband electron gas. In most of the calculations we have presented here we have somewhat arbitrarily chosen some adequate quasi-Fermi-energy level and it was assumed an homogeneous distribution of impurities along the QW, although we are aware that this may not be the case in some of the experimental situations. We do believe that more theoretical work is needed to achieve a complete quantitative description of the experimental data.

#### ACKNOWLEDGMENTS

We are grateful to M. de Dios Leyva for a critical reading of the manuscript. J. L-G. would like to thank the Brazilian Agency CNPq for partial financial support. This work was partially financed by Brazilian agencies Conselho Nacional de Desenvolvimento Científico e Tecnológico (CNPq), Financiadora de Estudos e Projetos (FINEP), and Fundação de Amparo e Pesquisa do Estado de Rio de Janeiro (FAPERJ).

- <sup>1</sup>L. Esaki and R. Tsu, I.B.M. Report No. R.C.-2418 (1969) (unpublished); I.B.M.J. Res. Dev. **14**, 61 (1970).
- <sup>2</sup>R. Dingle, in *Festkörperprobleme XV*, edited by H. J. Queisser (Pergamon, Braunschweig, 1975), p. 21.
- <sup>3</sup>L. Esaki, in *Recent Topics in Semiconductors Physics*, edited by H. Kamimura and Y. Toyozawa (World Scientific, Singapore, 1983), p. 1.
- <sup>4</sup>G. Bastard, J. Lumin. **30**, 488 (1985).
- <sup>5</sup>K. von Klitzing, G. Dorda, and M. Pepper, Phys. Rev. Lett. **45**, 494 (1980); D. C. Tsui and A. C. Gossard, Appl. Phys. Lett. **38**, 550 (1981).
- <sup>6</sup>D. C. Tsui, H. L. Stormer, and A. C. Gossard, Phys. Rev. Lett. **48**, 1559 (1982).
- <sup>7</sup>R. B. Laughlin, Phys. Rev. Lett. **50**, 1395 (1983).
- <sup>8</sup>R. C. Miller, D. A. Kleinman, and A. C. Gossard, Phys. Rev. B **29**, 7085 (1984).
- <sup>9</sup>W. Wang, E. E. Mendez, and F. Stern, Appl. Phys. Lett. **45**, 639 (1984).
- <sup>10</sup>J. P. van der Ziel, R. Dingle, R. C. Miller, W. Wiegmann, and W. A. Nordland, Jr., Appl. Phys. Lett. **26**, 463 (1975).
- <sup>11</sup>R. Dingle, H. L. Stormer, A. C. Gossard, and W. Wiegmann, Appl. Phys. Lett. **33**, 665 (1978).
- <sup>12</sup>J. N. Schulman and T. C. McGill, Appl. Phys. Lett. **34**, 663 (1979).
- <sup>13</sup>A. C. Gossard, Inst. Phys. Conf. Ser. **69**, 1 (1983).
- <sup>14</sup>N. T. Linh, Inst. Phys. Conf. Ser. **69**, 15 (1983).
- <sup>15</sup>S. Tarucha and H. Okamoto, Appl. Phys. Lett. **48**, 1 (1986).
- <sup>16</sup>G. Bastard, Phys. Rev. B **24**, 4714 (1981).
- <sup>17</sup>R. L. Greene and K. K. Bajaj, Solid State Commun. **45**, 825 (1983).
- <sup>18</sup>C. Mailhot, Y-C. Chang, and T. C. McGill, Phys. Rev. B **26**, 4449 (1982).
- <sup>19</sup>S. Chaudhuri and K. K. Bajaj, Phys. Rev. B **29**, 1803 (1984).
- <sup>20</sup>W. T. Masselink, Y-C. Chang, and H. Morkoç, Phys. Rev. B **28**, 7373 (1983).
- <sup>21</sup>W. T. Masselink, Y-C. Chang, and H. Morkoç, J. Vac. Sci. Technol. B **2**, 376 (1984); Phys. Rev. B **32**, 5190 (1985).
- <sup>22</sup>P. Csavinszky and A. M. Elabasy, Phys. Rev. B **32**, 6498 (1985).
- <sup>23</sup>L. E. Oliveira and L. M. Falicov, Phys. Rev. B **34**, 8676 (1986).
- <sup>24</sup>L. E. Oliveira, Phys. Rev. B **38**, 10641 (1988); Superlatt. Microstruct. **5**, 23 (1989).
- <sup>25</sup>R. C. Miller, A. C. Gossard, W. T. Tsang, and O. Munteanu, Phys. Rev. B **25**, 3871 (1982).
- <sup>26</sup>R. C. Miller, A. C. Gossard, W. T. Tsang, and O. Munteanu, Solid State Commun. **43**, 519 (1982).
- <sup>27</sup>M. H. Meynadier, J. A. Brum, C. Delalande, and M. Voos, J. Appl. Phys. **58**, 4307 (1985).
- <sup>28</sup>B. V. Shanabrook and J. Comas, Surf. Sci. **142**, 504 (1984).
- <sup>29</sup>B. V. Shanabrook, J. Comas, T. A. Perry, and R. Merlin, Phys. Rev. B **29**, 7096 (1984).
- <sup>30</sup>R. L. Greene and K. K. Bajaj, Solid State Commun. **53**, 1103 (1985).
- <sup>31</sup>C. Delalande, Physica B+C **146B**, 112 (1987).
- <sup>32</sup>B. V. Shanabrook, Physica B+C **146B**, 121 (1987).
- <sup>33</sup>Y-C. Chang, Physica B+C **146B**, 137 (1987).
- <sup>34</sup>Y-C. Chang, J. Phys. (Paris) Colloq. **48**, C5-373 (1987).
- <sup>35</sup>L. E. Oliveira and J. Lopez-Gondar, Appl. Phys. Lett. **55**, 275 (1989).
- <sup>36</sup>F. Bassani and G. Pastori Parravicini, in *Electronic States and Optical Transitions in Solids*, edited by R. A. Ballinger (Pergamon, Oxford, 1975).
- <sup>37</sup>R. Pérez-Alvarez and P. Pajón-Suarez, Phys. Status Solidi B **147**, 547 (1988).
- <sup>38</sup>B. A. Vojak, W. D. Laidig, N. Holonyak, Jr., M. D. Camras, J. J. Coleman, and P. D. Dapkus, J. Appl. Phys. **52**, 621 (1981).
- <sup>39</sup>L. E. Oliveira and R. Pérez-Alvarez, Solid State Commun. **70**, 523 (1989); Phys. Rev. B **40**, 10460 (1989).
- <sup>40</sup>H. C. Casey, Jr., J. Appl. Phys. **49**, 3684 (1978).
- <sup>41</sup>D. Chattopadhyay and A. Bhattachayra, Phys. Rev. B **37**, 7105 (1988).
- <sup>42</sup>W. Cai, T. F. Zheng, and M. Lax, Phys. Rev. B **37**, 8205 (1988).
- <sup>43</sup>S. K. Lyo and E. D. Jones, Phys. Rev. B **38**, 4113 (1989).
- <sup>44</sup>One should note that Meynadier *et al.* (Ref. 27) have assumed a Boltzmann law (with a  $T = 2$  K effective temperature) instead of a Fermi-Dirac one for the conduction-subband electronic distribution.